Environmental Science and Ecotechnology 22 (2024) 100452

Contents lists available at ScienceDirect

Environmental Science and Ecotechnology

journal homepage: www.journals.elsevier.com/environmental-science-and-ecotechnology/

Original Research

Kinetics and mechanisms of non-radically and radically induced degradation of bisphenol A in a peroxymonosulfate-chloride system

Zhao Song [a, b], Yu Zhang [a], Yanhu Yang [a], Yidi Chen [a, c, *], Nanqi Ren [a], Xiaoguang Duan [c]

[a] State Key Laboratory of Urban Water Resource and Environment, Shenzhen Key Laboratory of Organic Pollution Prevention and Control, School of Civil and Environmental Engineering, Harbin Institute of Technology (Shenzhen), Shenzhen, 518055, PR China
[b] School of Materials and Environmental Engineering, Shenzhen Polytechnic University, Shenzhen, 518055, PR China
[c] School of Chemical Engineering, The University of Adelaide, Adelaide, SA, 5005, Australia

ARTICLE INFO

Article history:
Received 13 November 2023
Received in revised form
3 July 2024
Accepted 5 July 2024

Keywords:
BPA removal
Saline wastewater
Peroxymonosulfate
Free chlorine
Kinetic model

ABSTRACT

Bisphenol A, a hazardous endocrine disruptor, poses significant environmental and human health threats, demanding efficient removal approaches. Traditional biological methods struggle to treat BPA wastewater with high chloride (Cl^-) levels due to the toxicity of high Cl^- to microorganisms. While persulfate-based advanced oxidation processes (PS-AOPs) have shown promise in removing BPA from high Cl^- wastewater, their widespread application is always limited by the high energy and chemical usage costs. Here we show that peroxymonosulfate (PMS) degrades BPA *in situ* under high Cl^- concentrations. BPA was completely removed in 30 min with 0.3 mM PMS and 60 mM Cl^-. Non-radical reactive species, notably free chlorine species, including dissolved Cl_2(l), HClO, and ClO^- dominate the removal of BPA at temperatures ranging from 15 to 60 °C. Besides, free radicals, including $^{\bullet}OH$ and $Cl_2^{\bullet-}$, contribute minimally to BPA removal at 60 °C. Based on the elementary kinetic models, the production rate constant of Cl_2(l) (32.5 M^{-1} s^{-1}) is much higher than HClO (6.5×10^{-4} M^{-1} s^{-1}), and its degradation rate with BPA (2×10^7 M^{-1} s^{-1}) is also much faster than HClO (18 M^{-1} s^{-1}). Furthermore, the degradation of BPA by Cl_2(l) and HClO were enlarged by 10- and 18-fold at 60 °C compared to room temperature, suggesting waste heat utilization can enhance treatment performance. Overall, this research provides valuable insights into the effectiveness of direct PMS introduction for removing organic micropollutants from high Cl^- wastewater. It further underscores the critical kinetics and mechanisms within the PMS/Cl^- system, presenting a cost-effective and environmentally sustainable alternative for wastewater treatment.

1. Introduction

In recent years, bisphenol A (BPA) has been widely used in the production of polymeric materials, such as polycarbonate, epoxy resins, polyacrylates, and polyvinyl chloride, with an estimated annual production of millions of tons per year [1,2]. BPA is a typical endocrine disruption compound that induces multiple endocrine diseases, including female and male infertility, precocious puberty, breast and prostate cancer, and polycystic ovarian syndrome, even at very low concentrations (ng L^{-1} to μg L^{-1}), due to its similar structure with estrogens [1,3]. Given its extensive utilization, it pervades our daily existence [3,4]. The release of BPA into natural waters through industrial and domestic wastewater discharges or landfill leachates threatens human health and the ecological system [4]. Polycarbonate plant wastewaters (PCW) are particularly problematic as they contain high levels of BPA and other recalcitrant organics, as well as considerable amounts of dissolved salts (e.g., 14,000 mg L^{-1} Cl^-) [5]. These micropollutants in saline water exhibit low biodegradability, leading to serious inhibition and toxicity to microorganisms and futility of biological treatment [1,6,7]. To address these challenges, researchers have explored using advanced oxidation processes for BPA degradation [8,9].

Among advanced oxidation processes, persulfate oxidation shows excellent potential for removing recalcitrant organic

* Corresponding author. State Key Laboratory of Urban Water Resource and Environment, Shenzhen Key Laboratory of Organic Pollution Prevention and Control, School of Civil and Environmental Engineering, Harbin Institute of Technology (Shenzhen), Shenzhen, 518055, PR China.
E-mail address: chenyidi@hit.edu.cn (Y. Chen).

https://doi.org/10.1016/j.ese.2024.100452

compounds. It is based on the activation of peroxymonosulfate (PMS, HSO_5^-) and peroxydisulfate (PDS, $S_2O_8^{2-}$) via radical and nonradical pathways. The radical pathway requires high-energy input [heat or ultraviolet (UV) irradiation] and/or catalysts (transition metals, non-metal catalysts, or alkaline) to break the peroxo bond and generate $SO_4^{\bullet-}$ and $^{\bullet}OH$ [10–12]. Although this method is relatively efficient, its practical application is limited by its high energy and chemical requirements. Compared to PDS [13,14], PMS is more readily activated by catalysts or inorganic anions due to its asymmetrical structure [8]. Techniques for activating PMS using halogens to produce active free halogen species [e.g., Cl_2(l)/HClO, $Cl_2^{\bullet-}$, $Br_2^{\bullet-}$, $I^{\bullet}$, and HOI] [7,8,15–18] have been studied. These halogen activation techniques can directly utilize the halogens in high-salinity wastewaters, such as Cl^-, thus avoiding additional chemicals or energy. However, research on Cl^- activation of PMS via radical or nonradical pathways for removing environmental contaminants is limited [19]. Previous studies have indicated that PMS can transfer oxygen atoms to some nucleophiles and form secondary oxidants (i.e., $HSO_5^- + X^- \rightarrow HSO_4^- + XO$, where X^- represents Cl^-, Br^-, and I^-), which can degrade pollutants [20]. As the synthetic of polycarbonates typically requires harsh reaction conditions (>200 °C) [21], rational utilization of waste heat is crucial for sustainable treatment of PCW in practical applications. Ahn et al. demonstrated that heat input can accelerate organic degradation and transform free chlorine into stronger oxidizing radicals via the PMS/Cl^- method [8]. However, the detailed kinetics of PMS activation by Cl^- and thermal acceleration have been barely reported, and the reaction rate constants between BPA and free chlorine or free radicals also require investigations to optimize the PMS/Cl^- system.

In this study, we directly activated PMS with high-concentration Cl^- referred to as real PCW to degrade BPA with no extra energy or chemical [5]. The enhancement of BPA removal at elevated temperatures and the detailed pathway involved at both the room and elevated temperatures were investigated. Although PMS activation by Cl^- and heat has been studied [8], few studies focused on the elementary reaction kinetics of the PMS/Cl^- and/or PMS/Cl^-/thermal processes. Therefore, based on experimental data from this study and the existing literature, two detailed kinetic models were established that consider a large family of relevant elementary reactions to describe the entire PMS/Cl^- and PMS/Cl^-/60 °C process. The models also consider the formation of $^1O_2$ under alkaline conditions in the PMS/Cl^- and PMS/Cl^-/60 °C processes. To evaluate the importance of various reactions in the model, principal component analysis (PCA) of the kinetic model was conducted. Our findings provide valuable insights into the activation and reaction capacities of PMS in removing BPA from high-salinity wastewaters, thus offering guidance for the practical application of direct PMS addition in PCW treatment.

2. Materials and methods

2.1. Chemicals and reagents

The chemical and reagent preparation procedures used in this study are listed in Section S1 of the Supplementary Materials.

2.2. Experimental procedures

The experiment used 100-mL beakers equipped with a magnetic stirrer at 500 rpm for 60 min. Reactions were initiated by adding PMS aliquots to the beakers. Sample aliquots (0.5 mL) were promptly taken for BPA detection and transferred to 2-mL vials that contained excess sodium thiosulfate ($[Na_2S_2O_3]/[PMS]_0 > 5$) to effectively quench any residual radicals. All experiments were duplicated and performed at room temperature (25 ± 2 °C) or under controlled temperatures (15, 30, 45, and 60 °C) using a thermostatically controlled water bath. Scavenging experiments were also conducted using scavengers, such as tert-butanol (TBA), methanol (MeOH), NH_4^+-N, or *p*-benzoquinone (p-BQ), at 30 mM.

2.3. Analytical methods

The BPA concentration was determined via ultra-performance liquid chromatography (UPLC, ACQUITY UPLC H-Class) equipped with a C18 column (2.1 × 100 mm) and a UV detector. The flow rate was 0.3 mL min^{-1}, and the mobile phase was a mixture of water (pH 3, adjusted using phosphoric acid) and acetonitrile (55/45, v/v%). The PMS consumption and the free chlorine production were measured with a Varian Cary 300 UV–visible (UV–vis) spectrometer. PMS was determined using the colorimetric method based on 2, 2′-azino-bis(3-ethylbenzothiazoline-6-sulfonic acid) radical ($ABTS^{\bullet+}$) (λ_{max} = 415 nm) production from ABTS oxidation by persulfate, with iodine compound catalyzing in an acetic acid buffer (pH 4) [22]. Total free chlorine, which included Cl_2(l), HClO, and ClO^-, was determined using the Hach Total Chlorine Method 8167, an Environmental Protection Agency-approved method based on the N, N-diethyl-*p*-phenylenediamine (DPD) method. The residual PMS was captured by excess ethylenediamine tetraacetic acid to inhibit the PMS interference [18,23]. Ionic chloride species, such as ClO^-, ClO_2^-, and ClO_3^-, were quantified via ion chromatography (Thermo Scientific, USA), which was equipped with a conductivity detector and used 23.3-mM KOH as effluent at a flow rate of 1 mL min^{-1} [8]. After a 1-h reaction, the products were analyzed using liquid chromatography–mass spectrometry (LC–MS, Triple Quad 4500, USA) equipped with a UPLC system and an electron spray ionization source.

2.4. Kinetic modeling

The observed reaction rate constants (k_{obs}) of the BPA degradation were determined using a pseudo-first-order kinetic equation with $R^2 > 0.9$ and empirical exponential function-based fits to the data. Kinetic modeling was performed using the Kintecus software, which can describe the concentrations of all the species present as functions of time and process conditions [24,25]. Two separate kinetic models were established for PMS/Cl^- at room temperature and at 60 °C to describe the experimental data under varying conditions. Kintecus conducted PCA of the kinetic model to calculate the normalized sensitivity coefficients and to evaluate the importance of reactions in the system [25,26]. To assess the contributions of various reactive species to the BPA removal, we assumed that different products corresponded to different reactive species, and we calculated the ratio of different products in the established kinetic model.

3. Results and discussion

3.1. BPA degradation by PMS/Cl^- at room temperature

The BPA degradation was negligible in the presence of pure PMS or Cl^-. However, when PMS and Cl^- were combined, BPA was significantly degraded (Supplementary Material Fig. S1). This indicates that PMS activation by Cl^- generates some reactive species that can degrade BPA. When the initial Cl^- and PMS dosages were increased, BPA removal was promoted (Fig. 1a and b). The k_{obs} of the BPA degradation was calculated based on the empirical exponential function-based fits. These rate constants were found to be proportional to the changes in the $[PMS]_0$ (from 0.1 to 0.5 mM; Supplementary Material Fig. S2) and the $[Cl^-]_0$ (from 20 to 100 mM;

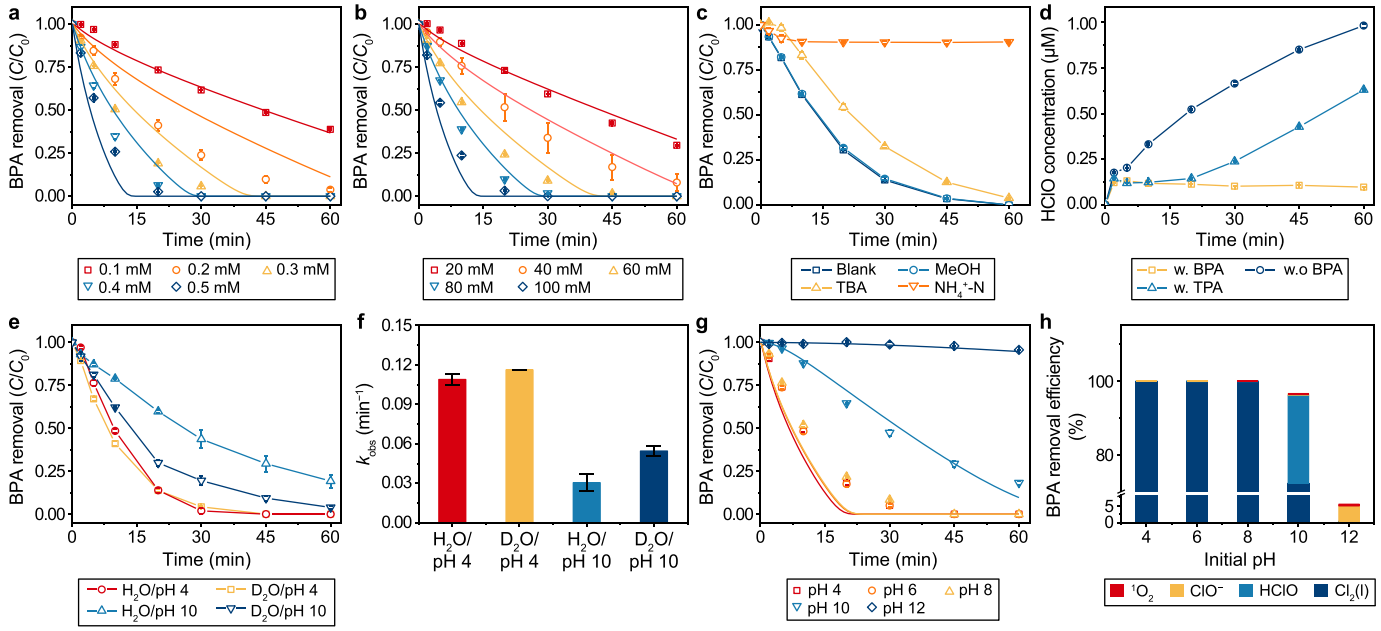

Fig. 1. **a**–**b**, BPA removal by PMS/Cl^- with a constant $[Cl^-]_0$ concentration of 60 mM and varying $[PMS]_0$ concentrations of 0.1, 0.2, 0.3, 0.4, and 0.5 mM (**a**) and a constant $[PMS]_0$ concentration of 0.3 mM and varying $[Cl^-]_0$ concentrations of 20, 40, 60, 80, and 100 mM (**b**). The symbols represent the experimental data ($n = 2$), and the lines represent the modeling results from Table S1 (Supplementary Materials). **c**, BPA removal by PMS/Cl^- in the presence of varying scavengers. **d**, Changes in the HClO concentration at varying conditions with BPA, without BPA, and with TBA, respectively. **e**–**f**, BPA removal (**e**) and k_{obs} (**f**) of the BPA removal in H_2O and D_2O solvent at the initial pH values of 4 and 10. **g**, BPA removal by PMS/Cl^- at varying pH values. **h**, Quantifying the reactive species responsible for the BPA removal efficiency at varying initial pH values based on the model in Table S1 (Supplementary Materials). Experiment conditions (unless stated otherwise): $[BPA]_0 = 0.01$ mM; $[PMS]_0 = 0.3$ mM; $[Cl^-]_0 = 60$ mM; [MeOH] = [TBA] = $[NH_4^+\text{-N}]$ = [p-BQ] = 30 mM.

Supplementary Material Fig. S3), which correspond to their real concentrations in the PCW [5], signifying that reactive species are proportionally produced in this homogeneous system.

To investigate the contributions of reactive species to BPA removal in the PMS/Cl^- system, common selective scavengers that have high rate constants with radicals ($k_{MeOH, {}^{\bullet}OH} = 9.7 \times 10^8$ M^{-1} s^{-1}, $k_{MeOH,SO_4^{\bullet-}} = 2.5 \times 10^7$ M^{-1} s^{-1}, $k_{TBA,{}^{\bullet}OH} = 3.8–7.6 \times 10^8$ M^{-1} s^{-1}, and $k_{TBA,\ SO_4^{\bullet-}} = 4.0–9.1 \times 10^5$ M^{-1} s^{-1}) were applied in excess (Fig. 1c). The results indicate that MeOH does not influence BPA removal, implying that $^{\bullet}OH$ or $SO_4^{\bullet-}$ is barely produced [8,27,28]. However, TBA exhibited slight suppression of BPA removal, suggesting the possible formation of other reactive species since the MeOH quenching result already excluded $^{\bullet}OH$. The absent removal of two probe compounds [benzoic acid (BA): $k_{BA, {}^{\bullet}OH} = 5.9 \times 10^9$ M^{-1} s^{-1}, $k_{BA, {}^{\bullet}Cl} = 1.8 \times 10^{10}$ M^{-1} s^{-1} (pH 4); and dimethyl phthalate (DMP): $k_{DMP, {}^{\bullet}OH} = 3.7 \times 10^9$ M^{-1} s^{-1}], as shown in Supplementary Material Fig. S4a, demonstrates that $^{\bullet}OH$ and $Cl^{\bullet}$ cannot be formed via Cl^- activation of PMS at room temperature [29].

Based on previous research, the asymmetric structure of PMS renders the peroxide bond highly vulnerable to nucleophilic attack by Cl^- [8]. PMS transfers oxygen atoms to Cl^- and yields highly selective oxidants [free chlorines, including Cl_2(l), HClO, and ClO^-] that tend to react with aromatic compounds containing electron-donating groups. Free chlorine has also been reported to be capable of substituting active hydrogen on the phenolic structure of BPA, forming chlorinated BPA congeners [30]. As NH_4^+-N can be transformed to NO_3^- by HClO, we used it as a free chlorine scavenger [31]. As shown in Fig. 1c, BPA removal was significantly inhibited to 7.9% with 30-mM NH_4^+-N, indicating that free chlorine was predominant in BPA removal in the PMS/Cl^- process at room temperature. The efficient degradation of the electron-rich organic compound *p*-aminobenzoic acid (*p*-ABA; $k_{p\text{-ABA, HClO}} = 4.3 \times 10^3$ M^{-1} s^{-1}) and the unaffected degradation of *p*-ABA in the presence of 30-mM MeOH (Supplementary Material Fig. S4b) also confirmed the selective contribution of HClO in the PMS/Cl^- process [8]. The HClO production was directly determined by the DPD method, as shown in Fig. 1d. In the absence of BPA, around 0.06-mM HClO was directly detected in the PMS/Cl^- process, but other oxychlorides, such as ClO_2^-, ClO_3^-, and ClO_4^-, were not observed (Supplementary Material Fig. S5). Over 0.05-mM free chlorine was consumed for BPA removal in the presence of 0.01-mM BPA (Fig. 1d), demonstrating that BPA was not only substituted once but that dichloride-, trichloride-, and tetrachloride-substituted BPA could also be produced. This was also verified by LC–MS. Fig. S6 (Supplementary Material) shows the products of BPA after a 1-h reaction, which reveal the existence of dichloro-substituted BPA, trichloro-substituted BPA, and other smaller molecules. Furthermore, in the absence of BPA, the addition of TBA significantly decreased the generation of free chlorine (Fig. 1d), suggesting that TBA could react with free chlorine and contributing to the suppressed BPA removal by TBA in Fig. 1c. In line with the previous discussion, free chlorine production and PMS consumption were accordingly accelerated by the increases in the PMS and Cl^- doses (Supplementary Material Fig. S7). Hence, free chlorine is the predominant reactive species for BPA removal in the PMS/Cl^- process at room temperature.

Other possible reactive oxygen species (ROS), such as $O_2^{\bullet-}$ and $^1O_2$, were excluded. As shown in Fig. S8 (Supplementary Material), no transformation of monoformazan from nitrotetrazolium blue was observed at 560 nm, suggesting that $O_2^{\bullet-}$ did not exist [32]. Regarding $^1O_2$, we replaced the deionized water with D_2O at the initial pH values of 4 and 10, as the half-lifetime of $^1O_2$ (1 μs) can be significantly extended in a D_2O environment (30–40 μs) [7]. As seen in Fig. 1e, BPA degradation was not improved in D_2O at pH 4, illustrating that $^1O_2$ is not the predominant ROS at pH 4. However, the BPA degradation efficiency and k_{obs} were significantly promoted in D_2O at pH 10 (Fig. 1e and f), implying the presence of $^1O_2$ under alkaline conditions, which is following previous research on

the generation of $^1O_2$ via the reaction between PMS and dissociated PMS (SO_5^{2-}) [27]. Additionally, we performed the BPA removal over a wide initial pH range of 4–12 in the PMS/Cl^- system. Due to the coexistence of HSO_4^- in PMS solutions, the solution pH gradually decreased to 3.5, 3.8, 3.8, 8.3, and 10.5 after a 60-min reaction at an initial pH of 4, 6, 8, 10, and 12, respectively. The BPA removal at an initial pH of 12 was significantly inhibited (Fig. 1g) due to the transformation of free chlorine species from Cl_2(l)/HClO [1.27–1.5 V vs. standard hydrogen electrode (SHE)] to ClO^- (0.9 V vs. SHE) [33]. Although $^1O_2$ is generated at alkaline conditions and can react rapidly with BPA (3×10^5 M^{-1} s^{-1}) and BPA^- (2×10^8 M^{-1} s^{-1}) [8], its production in this study was limited and insufficient to degrade BPA at an initial pH of 12. As shown in Fig. 1h, dissolved Cl_2(l) and HClO served as the predominant reactive species for BPA removal at the initial pH values of 4–8 and 10, respectively. At an initial pH of 12, however, the removal efficiency of BPA was only 5.3%, and the HClO, ClO^-, and $^1O_2$ contributions were 0.5%, 4.4%, and 0.4%, respectively.

3.2. BPA degradation by PMS/Cl^- at varying temperatures

To rationally utilize the waste heat from PCW [21], we investigated PMS activation by Cl^- promoted by heat. In Fig. 2a, BPA removal by pure PMS was negligible at temperatures of 15, 30, and 45 °C, but gradual degradation was observed when the temperature increased to 60 °C, indicating the initiation of a different BPA degradation pathway via thermal PMS activation. When 60-mM Cl^- was added to 0.3-mM PMS, the BPA removal rates were significantly enhanced with increasing temperatures, as shown in Fig. 2b. The correlation between k_{obs} and temperature is described by the Arrhenius equation ($\ln k_{obs} = -\frac{E_a}{R}\frac{1}{T} + C$) [34], yielding an E_a of 8.1 kJ mol^{-1}. This relatively low E_a value indicates that BPA degradation is readily achievable in the PMS/Cl^- process through the chlorine substitution reaction.

Scavenging experiments using MeOH, TBA, and NH_4^+-N were conducted at varying temperatures (Fig. 2c). The results show similar k_{obs} of BPA removal between the control without scavengers and the result with MeOH at 15, 30, and 45 °C, indicating no formation of free radicals. Moreover, the almost complete suppression of the BPA removal by NH_4^+-N at 15–45 °C demonstrates that free chlorine is predominant in BPA removal. At 60 °C, the suppression effect of NH_4^+-N was abated (Fig. 2c), and MeOH also exhibited inhibition of BPA removal, suggesting the formation of free radicals (such as •OH, $SO_4^{\bullet-}$, and Cl•) in the PMS/Cl^- process. Additionally, the consumption of PMS and the generation of free chlorine also increased with temperature (Fig. 3a and b). The concentration of HClO initially increased and then gradually declined at 60 °C (Fig. 3b), suggesting that HClO may be consumed to produce other reactive species.

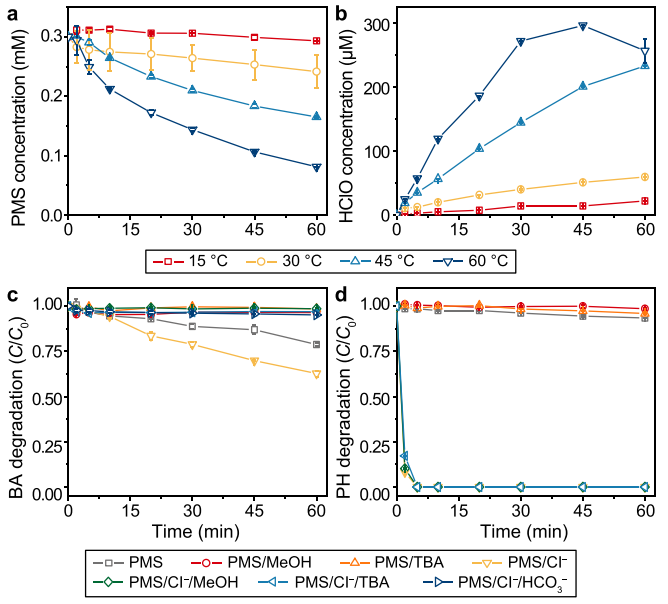

Fig. 3. **a**–**b**, PMS consumption (**a**) and HClO generation (**b**) with a $[Cl^-]_0$ concentration of 60 mM and a $[PMS]_0$ concentration of 0.3 mM without BPA during the process. **c**–**d**, The effects of ROS scavengers on BA (**c**) and PH (**d**) degradation by pure PMS and PMS/Cl^- at 60 °C.

Further experiments were conducted to identify the reactive species involved in the degradation of BA in pure PMS and a PMS/Cl^- system at different temperatures, along with scavenging experiments. Note that BA is a typical probe compound for •OH ($k_{BA,\bullet OH} = 5.9 \times 10^9$ M^{-1} s^{-1}), $SO_4^{\bullet-}$ ($k_{BA,SO_4^{\bullet-}} = 1.2 \times 10^9$ M^{-1} s^{-1}), and Cl• ($k_{BA,\bullet Cl} = 1.8 \times 10^{10}$ M^{-1} s^{-1}), but it is inert to free chlorine [8]. Fig. S9a (Supplementary Materials) shows that pure PMS degraded approximately 21% of BA at 60 °C, indicating the production of •OH, $SO_4^{\bullet-}$, or Cl• through a thermally activated process [8]. In the PMS/Cl^- systems at 15, 30, and 45 °C, although the generation of free chlorine was thermally enhanced (Fig. 3b), BA could not be degraded (Supplementary Material Fig. S9b) [35]. However, the addition of Cl^- accelerated the BA removal in the PMS/60 °C system, possibly due to the generation of Cl• by the reactions between Cl^- and •OH/$SO_4^{\bullet-}$, which exhibited a higher reaction rate with BA [8]. To ascertain the role of Cl• in BA removal, HCO_3^-, which selectively scavenges Cl• ($k_{HCO_3^-,\bullet OH} = 8.5 \times 10^6$ M^{-1} s^{-1}, $k_{HCO_3^-,SO_4^{\bullet-}} = 9.1 \times 10^6$ M^{-1} s^{-1}, and $k_{HCO_3^-,\bullet Cl} = 2.4 \times 10^9$ M^{-1} s^{-1}), was applied to the PMS/Cl^-/60 °C system [36,37]. The results show that adding HCO_3^- significantly inhibited BA removal (Fig. 3c), demonstrating the thermally initiated generation of Cl• [8]. MeOH and TBA completely hindered BA degradation at 60 °C in both pure PMS and

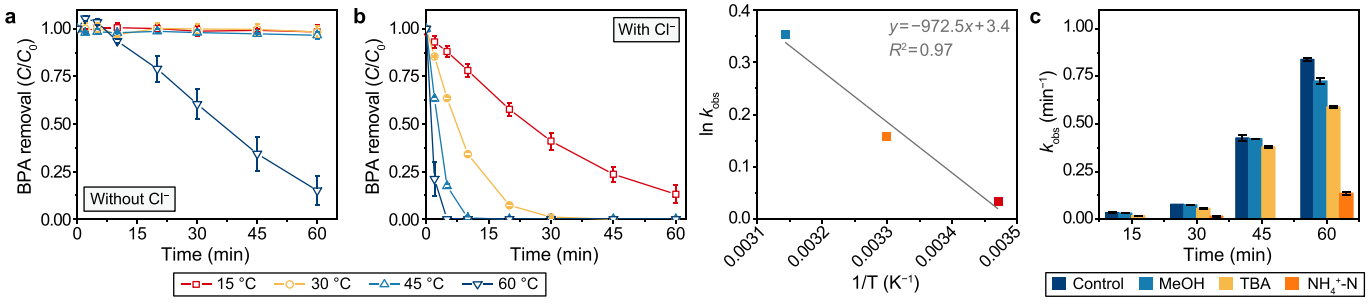

Fig. 2. **a**–**b**, Changes in BPA removal at the initial BPA concentration of 0.01 mM by PMS with (**a**) or without (**b**) Cl^- at controlled temperatures of 15, 30, 45, and 60 °C. The subgraph represents the correlation between ln k_{obs} and 1/*T*. **c**, Observed reaction rate constants of the BPA removal quenched by MeOH, TBA, and NH_4^+-N at elevated temperatures.

the PMS/Cl^- processes (Fig. 3c), confirming the crucial role of $^{\bullet}OH$, $SO_4^{\bullet-}$, or $Cl^{\bullet}$ in BA degradation. Previous studies have reported that $^{\bullet}OH$ can transform BA to *p*-HBA, and $SO_4^{\bullet-}$ can transform *p*-HBA to p-BQ [38,39]. Indeed, small amounts of *p*-HBA and p-BQ were detected (Supplementary Material Figs. S10a–b), certifying the presence of $^{\bullet}OH$ and $SO_4^{\bullet-}$.

In Fig. 3d, phenol (PH), a compound susceptible to radicals and free chlorine, was assessed at 60 °C [8]. While pure PMS could degrade a small amount of PH, the PMS/Cl^- process completely decomposed it. MeOH and TBA completely scavenged the reaction in the pure PMS process, but only minimal quenching was observed in the PMS/Cl^- process, suggesting two different degradation pathways [8]. First, the thermally activated PMS produced free radicals, although insufficient for efficient PH degradation due to the limited PMS dosage or the existence of other potential sinks for free radicals, such as HSO_4^- ($k_{HSO_4^-,{}^{\bullet}OH} = 6.9 \times 10^5\ M^{-1}\ s^{-1}$). Second, the Cl^--mediated activation of PMS that induces free chlorine was thermally promoted, as measured in Fig. 3b, leading to the enhancement of the PH degradation.

3.3. Kinetic modeling of BPA degradation by PMS/Cl^- and PMS/Cl^-/60 °C

Two comprehensive kinetic modeling were developed based on the experimental results and the reported literature to investigate the activation rates of PMS through various pathways and the reaction rate constants between BPA and free chlorine, free radicals, and $^1O_2$. The elementary reaction rate constants depended solely on temperature and remained unaffected by the reactant concentrations or the solution pH. Accordingly, two separate theoretical models were constructed for the PMS/Cl^- and PMS/Cl^-/60 °C processes based on the assumptions outlined in Section S2, with the detailed modeling process illustrated in Section S2 and the results summarized in Tables S1 and S2 (Supplementary Materials).

3.3.1. Proposed PMS/Cl^- kinetic model

In the PMS/Cl^- process at room temperature, free chlorine species, including dissolved Cl_2(l), HClO, and ClO^-, act as the predominant ROS, producing no other oxidants. The significance of dissolved Cl_2(l) in the degradation of organics has often been overlooked due to its low concentrations in solutions, which was elucidated in this model. To calculate the reaction rate constants between BPA and free chlorine species, direct degradation of 0.01-mM BPA by HClO, HclO/Cl^-, and ClO^- was conducted, as shown in Fig. S11 (Supplementary Materials). Based on the kinetic model, the production rate of Cl_2(l) (Reactions 19 and 20, $k_{PMS,Cl^-} = 32.5\ M^{-1}\ s^{-1}$ and $k_{SO_5^{2-},Cl^-} = 3.25 \times 10^{-2}\ M^{-1}\ s^{-1}$) is much faster than that of HClO (Reactions 17 and 18, $k_{PMS,Cl^-} = 6.5 \times 10^{-4}\ M^{-1}\ s^{-1}$ and $k_{SO_5^{2-},Cl^-} = 6.5 \times 10^{-6}\ M^{-1}\ s^{-1}$), which is consistent with previous research [40]. Moreover, the reaction rate constant of BPA degradation by Cl_2(l) (Reaction 35, $k_{BPA,Cl_2} = 2 \times 10^7\ M^{-1}\ s^{-1}$) is also significantly higher than that by HClO (Reaction 23, $k_{BPA,HClO} = 18\ M^{-1}\ s^{-1}$).

3.3.2. Proposed PMS/Cl^-/60 °C kinetic model

In the PMS/Cl^-/60 °C process, we established another model (shown in Supplementary Material Table S2) to investigate the generation and consumption of free chlorine, radicals, and $^1O_2$. It is well known that the acid dissociation and volatilization reactions are endothermic reactions and that heat can significantly increase the rate constants of these reactions. Therefore, we amplified the acid–base equilibrium constants (Reactions 1–14, Supplementary Material Table S2) based on Table S1 (Supplementary Materials) and the experimental data in Fig. 4a–f and Supplementary Material Figs. S11–S15 [8]. Before studying the thermally activated pathways of PMS with Cl^-, we first examined the BPA removal efficiency under different free chlorine species accelerated at 60 °C (Supplementary Material Fig. S11b). Based on the experimental data in Fig. S11b (Supplementary Materials), the equilibrium constants in Reactions 3–8 and the rate constants in Reactions 71–77 and 84–90 were determined. The reaction rate constants for BPA with HClO ($k_{BPA,HClO} = 1.8 \times 10^2\ M^{-1}\ s^{-1}$), ClO^- ($k_{BPA,ClO^-} = 1.1 \times 10^2\ M^{-1}\ s^{-1}$), and Cl_2 ($k_{BPA,Cl_2\ (l)} = 2.0 \times 10^8\ M^{-1}\ s^{-1}$) were calculated at 60 °C, which were approximately 10, 7.7, and 10 times higher, respectively, than those at room temperature. However, the evaporation rate constant of Cl_2(g) from dissolved Cl_2(l) was also promoted, reducing the exposure of BPA to dissolved Cl_2(l) and leading to a similar BPA removal efficiency rate with or without 60-mM Cl^-, as shown in Fig. S11b (Supplementary Materials). Subsequently, the BPA removal and the PMS consumption in the PMS/60 °C without a Cl^- treatment process were evaluated (Supplementary Material Fig. S12) to define the rate of $^{\bullet}OH$ and $SO_4^{\bullet-}$ generated from the PMS decomposition (Reaction 18). As stated in the assumptions, the oxidation rates of BPA by $^{\bullet}OH$ and $SO_4^{\bullet-}$ (Reactions 66–67) directly referred to the reported study at room temperature [8,27]. In the PMS/Cl^-/60 °C solutions, the generated $^{\bullet}OH$ and $SO_4^{\bullet-}$ not only removed the BPA but also participated in the chain reactions with multiple anions and radicals, as described in Reactions 24–64 [41]. When Cl^- was added, $Cl^{\bullet}$, $Cl_2^{\bullet-}$, and $ClO^{\bullet}$ were formed by the reaction of Cl^- with $^{\bullet}OH$ and $SO_4^{\bullet-}$, which enhanced the BPA and BA degradation (Reaction 68, $k_{BPA,Cl^{\bullet}} = 1.82 \times 10^{10}\ M^{-1}\ s^{-1}$; Reaction 69, $k_{BPA,Cl_2^{\bullet-}} = 5.82 \times 10^8\ M^{-1}\ s^{-1}$; and Reaction 70,

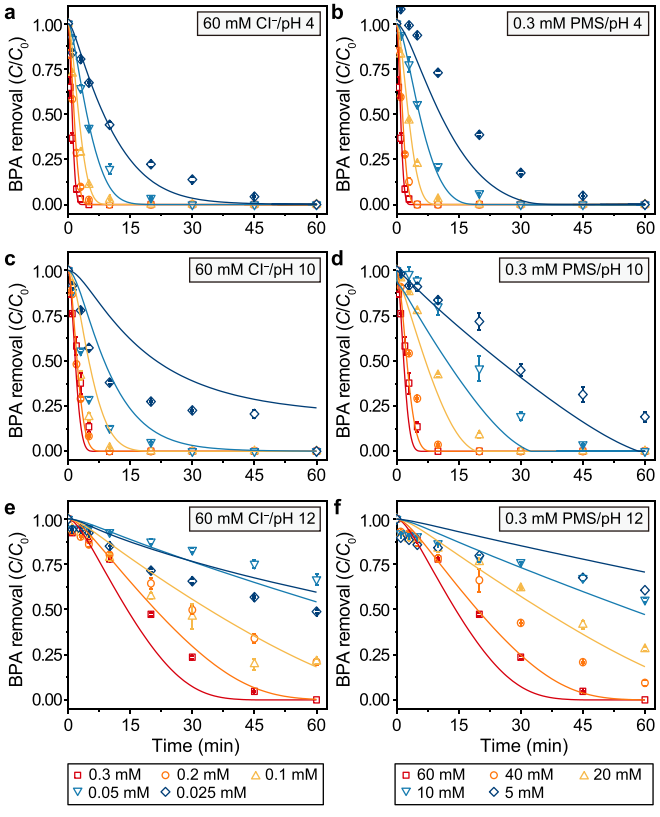

Fig. 4. Changes in the C/C_0 of 0.01-mM BPA by PMS/Cl^-/60 °C with a constant $[Cl^-]_0$ concentration of 60 mM and varying $[PMS]_0$ concentrations at the initial pH 4 (**a**), pH 10 (**c**), and pH 12 (**e**) values, and a constant $[PMS]_0$ concentration of 0.3 mM and varying $[Cl^-]_0$ concentrations at the initial pH 4 (**b**), pH 10 (**d**), and pH 12 (**f**) values. The symbols represent the experimental data ($n = 2$), and the lines represent the modeling results from Table S2 (Supplementary Materials).

$k_{BPA,ClO^{\bullet}} = 1 \times 10^8\ M^{-1}\ s^{-1}$, respectively) in the PMS/Cl^-/60 °C system.

In Fig. 4 and Supplementary Material Figs. S13–S15, the kinetic model describes the overall BPA removal trend with varying PMS and Cl^- dosages and pH values. The production rate constants of HClO and $^1O_2$ by PMS and Cl^- were enlarged 18- and 30-fold after heat acceleration, compared to room temperature. However, due to the limited concentration of 0.3-mM PMS, the populated $^1O_2$ could not significantly enhance the BPA removal under pH 12. To estimate the oxidation rates of dissociated BPA^- species by different reactive species, as shown in Fig. S15 (Supplementary Materials) at an initial pH of 12, the rate constants for Reactions 78–90 were calculated, and BPA^- exhibited higher reaction rate constants than BPA. Based on the model in Supplementary Material Table S2, $Cl_2^{\bullet-}$ and $^{\bullet}OH$ contributed approximately 1.1% and 0.2% BPA removal efficiencies at an initial pH of 4 and 2.1% and 0.5% at an initial pH of 10, respectively. $^1O_2$ accounted for 1.1% BPA removal at an initial pH of 12. Other radicals, including $SO_4^{\bullet-}$, $Cl^{\bullet}$, and $ClO^{\bullet}$, also existed in the system but had negligible effects on BPA removal and, thus, are not shown in Fig. S16 (Supplementary Materials). Free chlorine species contributed to the rest of the BPA removal and gradually transformed from Cl_2(l) to HClO and ClO^- at initial pH values of 4–12.

Although the kinetic model describes the overall trend of BPA removal, there were discrepancies between the predicted results and the experimental data. In the case of 5-mM Cl^- and 0.3-mM PMS, the predicted results overestimated the BPA degradation. This discrepancy may be attributed to the neglected competition of intermediates from the BPA degradation for the limited free chlorine. The model predictions and the experimental data had further discrepancies under pH 10 and 12, as shown in Fig. 4c–f, possibly due to differences between the actual situations and the assumed and simplified models. Many reactions in PMS/Cl^-/60 °C were not considered here because a unique solution for the model is not feasible. We intended to constrain the mechanistic possibilities using the reasonable values in Table S2 (Supplementary Materials).

3.3.3. Principal component analysis of the kinetic model

In the kinetic model for BPA degradation by PMS/Cl^- at room temperature and 60 °C, PCA analysis was conducted to identify the critical reactions (Supplementary Material Fig. S17). The results (Supplementary Material Table S3) showed five critical reactions at room temperature and nine critical reactions at 60 °C. These reactions play a significant role in the BPA degradation process.

At room temperature, the dominant reactive species is free chlorine, especially dissolved Cl_2(l). Therefore, in this kinetic model, the reversible reactions between Cl_2(l) and HClO, the PMS activation by Cl^- to generate Cl_2(l) and HClO, and the monochloride substitution of BPA by Cl_2(l) and HClO are considered significant reactions. For the reactions in PMS/Cl^-/60 °C, in addition to the reversible reactions between Cl_2(l) and HClO, other significant reactions include the HClO decomposition, the PMS activation by Cl^- to generate HClO and the monochloride substitution of BPA by Cl_2(l). The thermal activation of PMS is also a significant reaction in this model, although $^{\bullet}OH$ and $SO_4^{\bullet-}$ have minor contributions to BPA degradation. The BPA degradation by $Cl_2^{\bullet-}$, the generation of $Cl_2^{\bullet-}$, and the generation and consumption of $Cl^{\bullet}$ are also significant for BPA removal; and the generation of massive chloride radicals in the PMS/Cl^-/60 °C system explains its higher BA removal capability than that of the PMS/Cl^- system. It should be noted that the remaining reactions in Tables S1 and S2 (Supplementary Materials) are intermediate reactions, which means that their rate constants may not significantly affect the overall BPA degradation, but their presence is still necessary to accurately describe the reaction mechanism.

4. Conclusion

In this study, we investigated BPA degradation using the PMS/Cl^- system at both room temperature and with heat activation. The asymmetric structure of PMS makes its peroxide bond susceptible to Cl^- attack, generating free chlorine [Cl_2(l), HClO, and ClO^-] to degrade BPA with products that include monochloride-, dichloride-, trichloride-, and tetrachloride-substituted BPA. Increasing the reaction temperature from 15 to 45 °C accelerated the production of free chlorine, the predominant reactive species, thereby more effectively degrading BPA. In the PMS/Cl^-/60 °C system, although the primary reactive species was free chlorine, the existence of radicals such as $^{\bullet}OH$, $SO_4^{\bullet-}$, and $Cl_2^{\bullet-}$ and their contribution to the BPA degradation were demonstrated. This suggests that these radicals, alongside free chlorine, can potentially enhance BPA removal efficiency. Further exploration and optimization of these radicals' generation and utilization could improve treatment strategies.

The established detailed kinetic models describing the PMS/Cl^- and PMS/Cl^-/60 °C processes are valuable tools for understanding the reaction mechanisms and kinetics involved in BPA degradation. In the kinetics study, the increase in the reaction temperature improved the PMS activation by Cl^- and enhanced the BPA oxidation rate by free chlorine. This implies that waste heat resources from industrial processes can be used to treat BPA-containing wastewater, improving the overall energy efficiency of the treatment process. These models can be further refined and utilized to optimize the treatment process and the design reactors, and to predict the BPA removal efficiency under different operating conditions.

Overall, this study highlights the potential of the PMS/Cl^- system with heat activation for efficiently removing BPA from wastewater. The findings open possibilities for utilizing waste heat, exploring radical contributions, optimizing treatment conditions, and developing kinetic models to advance BPA degradation technologies. These prospects have implications for developing more sustainable and effective methods of treating BPA-contaminated high-salinity wastewater.

CRediT authorship contribution statement

Zhao Song: Data Curation, Methodology, Software, Validation, Writing - Original Draft, Writing - Review & Editing. **Yu Zhang:** Investigation, Methodology, Visualization. **Yanhu Yang:** Investigation. **Yidi Chen:** Conceptualization, Funding Acquisition, Resources, Supervision, Validation, Writing - Review & Editing. **Nanqi Ren:** Funding Acquisition, Supervision, Writing - Review & Editing. **Xiaoguang Duan:** Writing - Review & Editing.

Declaration of competing interest

The authors declare that they have no known competing financial interests or personal relationships that could have appeared to influence the work reported in this paper.

Acknowledgments

We acknowledge the financial support provided by the fellowship of the Key-Area Research and Development Program of Guangdong Province (No. 2023B0101200004), the Shenzhen Science and Technology Innovation Program (No. RCBS20210706092219047, GXWD20231129122140001, KQTD20190929172630447, 2022A1515110698, and RCBS 20221008093229033), the National Natural Science Foundation of China (No. 52000053), and the Open Project of State Key Laboratory

of Urban Water Resources and Environment (QA202440).

Appendix A. Supplementary data

Supplementary data to this article can be found online at https://doi.org/10.1016/j.ese.2024.100452.

References

[1] S.A. Mirzaee, N. Jaafarzadeh, S. Jorfi, H.T. Gomes, M. Ahmadi, Enhanced degradation of Bisphenol A from high saline polycarbonate plant wastewater using wet air oxidation, Process Saf. Environ. 120 (2018) 321–330.

[2] R.D. Huelsmann, C. Will, E. Carasek, Determination of bisphenol A: Old problem, recent creative solutions based on novel materials, J. Sep. Sci. 44 (2021) 1148–1173.

[3] W. Liu, H. Zhang, B. Cao, K. Lin, J. Gan, Oxidative removal of bisphenol A using zero valent aluminum-acid system, Water Res. 45 (2021) 1872–1878.

[4] Y. Liu, S. Zhang, N. Song, R. Guo, M. Chen, D. Mai, Z. Yan, Z. Han, J. Chen, Occurrence, distribution and sources of bisphenol analogues in a shallow Chinese freshwater lake (Taihu Lake): implications for ecological and human health risk, Sci. Total Environ. 599–600 (2017) 1090–1098.

[5] J. Pan, B. Gao, Y. Gao, P. Duan, K. Guo, M. Akram, X. Xu, Q. Yue, In-situ Cu-doped carbon-supported catalysts applied for high-salinity polycarbonate plant wastewater treatment and a coupling application, Chem. Eng. J. 416 (2021) 129441.

[6] P. Guerra, M. Kim, S. Teslic, M. Alaee, S.A. Smyth, Bisphenol-A removal in various wastewater treatment processes: operational conditions, mass balance, and optimization, J. Environ. Manage. 152 (2015) 192–200.

[7] R. Luo, M. Li, C. Wang, M. Zhang, M.A. Nasir Khan, X. Sun, J. Shen, W. Han, L. Wang, J. Li, Singlet oxygen-dominated non-radical oxidation process for efficient degradation of bisphenol A under high salinity condition, Water Res. 148 (2019) 416–424.

[8] Y.Y. Ahn, J. Choi, M. Kim, M.S. Kim, D. Lee, W.H. Bang, E.T. Yun, H. Lee, J.H. Lee, C. Lee, S.K. Maeng, S. Hong, J. Lee, Chloride-mediated enhancement in heat-induced activation of peroxymonosulfate: New reaction pathways for oxidizing radical production, Environ. Sci. Technol. 55 (2021) 5382–5392.

[9] K. Li, S. Xu, X. Liu, H. Li, S. Zhan, S. Ma, Y. Huang, S. Liu, X. Zhuang, The organic contaminants degradation in Mn-NRGO and peroxymonosulfate system: the significant synergistic effect between Mn nanoparticles and doped nitrogen, Chem. Eng. J. 438 (2022) 135630.

[10] Y.H. Guan, J. Ma, X.C. Li, J.Y. Fang, L.W. Chen, Influence of pH on the formation of sulfate and hydroxyl radicals in the UV/peroxymonosulfate system, Environ. Sci. Technol. 45 (2011) 9308–9314.

[11] L. Jin, S. You, N. Ren, B. Ding, Y. Liu, Mo vacancy-mediated activation of peroxymonosulfate for ultrafast micropollutant removal using an electrified mXene filter functionalized with Fe single atoms, Environ. Sci. Technol. 56 (2022) 11750–11759.

[12] M. Li, S. You, X. Duan, Y. Liu, Selective formation of reactive oxygen species in peroxymonosulfate activation by metal-organic framework-derived membranes: a defect engineering-dependent study, Appl. Catal. B Environ. 312 (2022) 121419.

[13] J. Yang, M. Zhu, D.D. Dionysiou, What is the role of light in persulfate-based advanced oxidation for water treatment? Water Res. 189 (2021) 116627.

[14] S. Yang, P. Wang, X. Yang, L. Shan, W. Zhang, X. Shao, R. Niu, Degradation efficiencies of azo dye Acid Orange 7 by the interaction of heat, UV and anions with common oxidants: persulfate, peroxymonosulfate and hydrogen peroxide, J. Hazard Mater. 179 (2010) 552–558.

[15] F. Liu, Z. Wang, S. You, Y. Liu, Electrogenerated quinone intermediates mediated peroxymonosulfate activation toward effective water decontamination and electrode antifouling, Appl. Catal. B Environ. 320 (2023) 121980.

[16] Y. Feng, P.H. Lee, D. Wu, K. Shih, Rapid selective circumneutral degradation of phenolic pollutants using peroxymonosulfate-iodide metal-free oxidation: role of iodine atoms, Environ. Sci. Technol. 51 (2017) 2312–2320.

[17] J. Li, J. Jiang, Y. Zhou, S.Y. Pang, Y. Gao, C. Jiang, J. Ma, Y. Jin, Y. Yang, G. Liu, L. Wang, C. Guan, Kinetics of oxidation of iodide (I^-) and hypoiodous acid (HOI) by peroxymonosulfate (PMS) and formation of iodinated products in the PMS/I^-/NOM system, Environ. Sci. Technol. 4 (2017) 76–82.

[18] C.X. Li, C.B. Chen, Y.J. Wang, X.Z. Fu, S. Cui, J.Y. Lu, J. Li, H.Q. Liu, W.W. Li, T.C. Lau, Insights on the pH-dependent roles of peroxymonosulfate and chlorine ions in phenol oxidative transformation, Chem. Eng. J. 362 (2019) 570–575.

[19] Y. Zhou, J. Jiang, Y. Gao, S.Y. Pang, J. Ma, J. Duan, Q. Guo, J. Li, Y. Yang, Oxidation of steroid estrogens by peroxymonosulfate (PMS) and effect of bromide and chloride ions: kinetics, products, and modeling, Water Res. 138 (2018) 56–66.

[20] B. Sheng, Y. Huang, Z. Wang, F. Yang, L. Ai, J. Liu, On peroxymonosulfate-based treatment of saline wastewater: when phosphate and chloride co-exist, RSC Adv. 8 (2018) 13865–13870.

[21] T. Abe, T. Kamiya, H. Otsuka, D. Aoki, Plastics to fertilizer: guiding principles for functionable and fertilizable fully bio-based polycarbonates, Polym. Chem. 14 (2023) 2469–2477.

[22] J. Zou, Y. Huang, L. Zhu, Z. Cui, B. Yuan, Multi-wavelength spectrophotometric measurement of persulfates using 2,2'-azino-bis(3-ethylbenzothiazoline-6-sulfonate) (ABTS) as indicator, Spectrochim. Acta 216 (2019) 214–220.

[23] R.F. Lane, C.D. Adams, S.J. Randtke, R.E. Carter, Chlorination and chloramination of bisphenol A, bisphenol F, and bisphenol A diglycidyl ether in drinking water, Water Res. 79 (2015) 68–78.

[24] J.C. Ianni, A comparison of the Bader-Deuflhard and the Cash-Karp Runge-Kutta integrators for the GRI-MECH 3.0 model based on the chemical kinetics code Kintecus, in: K.J. Bathe (Ed.), Computational Fluid and Solid Mechanics 2003, Elsevier Science Ltd, Oxford, 2003, pp. 1368–1372.

[25] Y. Chen, C.J. Miller, T.D. Waite, Heterogeneous Fenton chemistry revisited: mechanistic insights from ferrihydrite-mediated oxidation of formate and oxalate, Environ. Sci. Technol. 55 (2021) 14414–14425.

[26] S. Vajda, P. Valko, T. Turanyi, Principal component analysis of kinetic models, Int. J. Chem. Kinet. 17 (1985) 55–81.

[27] J. Lee, U. von Gunten, J.H. Kim, Persulfate-based advanced oxidation: critical assessment of opportunities and roadblocks, Environ. Sci. Technol. 54 (2020) 3064–3081.

[28] S. Li, J. Huang, X. Li, L. Li, The relation of interface electron transfer and PMS activation by the H-bonding interaction between composite metal and MCM-48 during sulfamethazine ozonation, Chem. Eng. J. 398 (2018) 125529.

[29] Y. Zhang, J. Li, J. Bai, L. Li, S. Chen, T. Zhou, J. Wang, L. Xia, Q. Xu, B. Zhou, Extremely efficient decomposition of ammonia N to N(2) using ClO(*) from reactions of HO(*) and HOCl generated in situ on a novel bifacial photoelectroanode, Environ. Sci. Technol. 53 (2019) 6945–6953.

[30] H. Gallard, A. Leclercq, J.P. Croue, Chlorination of bisphenol A: kinetics and by-products formation, Chemosphere 56 (2004) 465–473.

[31] W. Kuang, Z. Yan, J. Chen, X. Ling, W. Zheng, W. Huang, C. Feng, A bipolar membrane-integrated electrochlorination process for highly efficient ammonium removal in mature landfill leachate: the importance of ClO(*) generation, Environ. Sci. Technol. 57 (2023) 18538–18549.

[32] X. Long, Z. Xiong, R. Huang, Y. Yu, P. Zhou, H. Zhang, G. Yao, B. Lai, Sustainable Fe(III)/Fe(II) cycles triggered by co-catalyst of weak electrical current in Fe(III)/peroxymonosulfate system: Collaboration of radical and non-radical mechanisms, Appl. Catal. B Environ. 317 (2022) 121716.

[33] C. Apua, Dissolution of low grade gold-bearing material with chloride/chlorine solution, in: Conference: 51st Annual Conference of Metallurgists of CIM (COM 2012)At: Niagara, ON, Canada, 2012.

[34] M.W. Zhang, M.T. Yang, S. Tong, K.A. Lin, Ferrocene-modified iron-based metal-organic frameworks as an enhanced catalyst for activating oxone to degrade pollutants in water, Chemosphere 213 (2018) 295–304.

[35] M. Deborde, U. von Gunten, Reactions of chlorine with inorganic and organic compounds during water treatment-Kinetics and mechanisms: a critical review, Water Res. 42 (2008) 13–51.

[36] Q. Yang, X. Niu, Y. Zhu, Y. Cui, Y. Chao, P. Liang, C. Zhang, S. Wang, Modulating anion defect in La(0.6)Sr(0.4)Co(0.8)Fe(0.2)O(3-delta) for enhanced catalytic performance on peroxymonosulfate activation: importance of hydrated electrons and metal-oxygen covalency, J. Hazard Mater. 432 (2022) 128686.

[37] K. Guo, Z. Wu, C. Shang, B. Yao, S. Hou, X. Yang, W. Song, J. Fang, Radical chemistry and structural relationships of PPCP degradation by UV/chlorine treatment in simulated drinking water, Environ. Sci. Technol. 51 (2017) 10431–10439.

[38] P. Cao, X. Quan, K. Zhao, S. Chen, H. Yu, Y. Su, High-efficiency electrocatalysis of molecular oxygen toward hydroxyl radicals enabled by an atomically dispersed iron catalyst, Environ. Sci. Technol. 54 (2020) 12662–12672.

[39] J. Criquet, N.K.V. Leitner, Reaction pathway of the degradation of the p-hydroxybenzoic acid by sulfate radical generated by ionizing radiations, Radiat. Phys. Chem. 106 (2015) 307–314.

[40] F.J. Rivas, R.R. Solís, Chloride promoted oxidation of tritosulfuron by peroxymonosulfate, Chem. Eng. J. 349 (2018) 728–736.

[41] K. Zhang, K.M. Parker, Halogen radical oxidants in natural and engineered aquatic systems, Environ. Sci. Technol. 52 (2018) 9579–9594.